

## Advances in high-precision lithium isotopic measurements with the Neoma™ MC-ICP-MS

Jouini A.<sup>1,\*</sup>, Payant L.<sup>1</sup>, Vigier N.<sup>1</sup>

### **Supplementary materials**

- I. MicroFAST Isotope I autosampler (*Elemental Scientific Inc.* (ESI), Omaha, USA): dual-loop wash optimization

*Classical dual loop system:*

The dual-loop injection system of the microFAST Isotope I autosampler is composed of two loops (A and B), two syringes, and two four-way valves (P4 and P4F).

- Step 1: The sample 1 solution (yellow pathway) contained in loop A is injected into the nebulizer for analysis, while loop B is simultaneously rinsed with the working solution (blue pathway in Figure. S1).
- Step 2: Loop A continues to deliver sample 1 to the nebulizer (yellow pathway), while loop B loads the next sample 2 solution (green pathway).
- Step 3: The two four-way valves switch positions, allowing sample 2 in loop B to be injected into the nebulizer (green pathway), while loop A is rinsed with the working solution (blue pathway).
- Step 4: The valves switch again loop B continues to inject sample 2 into the nebulizer (green pathway), while loop A loads the new sample 3 solution (green pathway).

This alternating sequence ensures a continuous sample introduction cycle, where one loop injects while the other is simultaneously cleaned and prepared, thereby maximizing analytical throughput

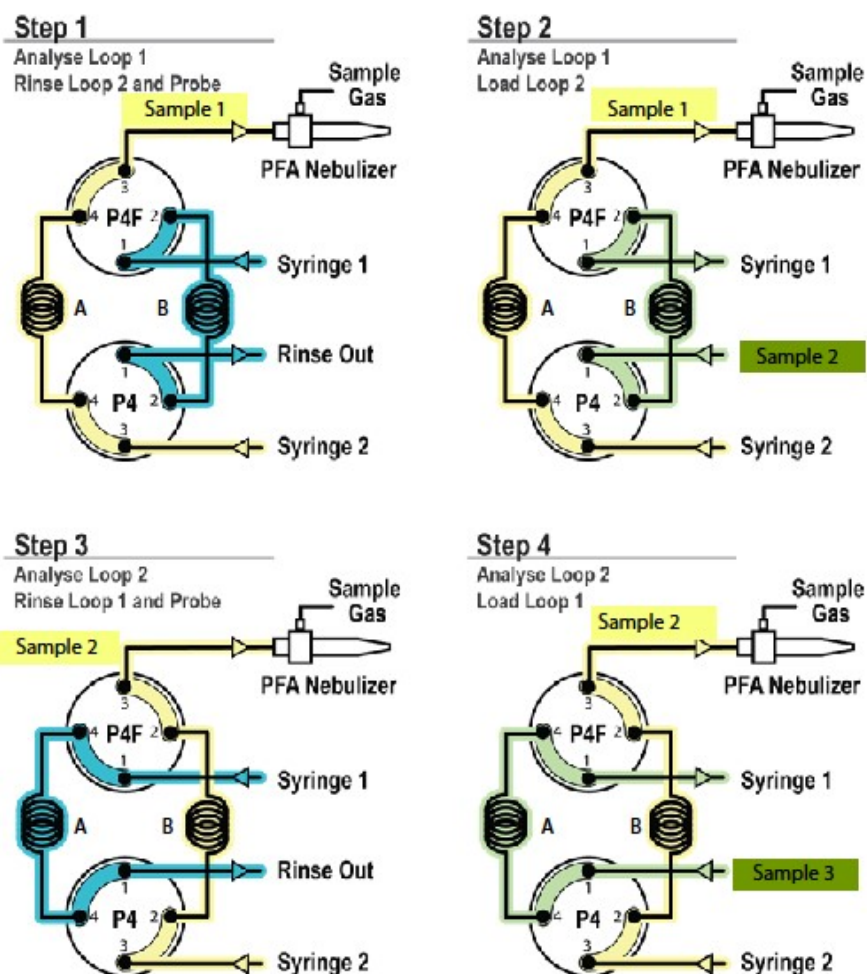


Figure S1: Schematic representation of the dual-loop dual-loop microFAST Isotope I autosampler sequence enabling continuous sample loading and analyses. Modified from <https://www.icpms.com/products/autosamplers-for-icp-icpms/>

When coupled with the standard Sample Standard Bracketing (SSB) method, the alternating dual-loop operation of the dual-loop microFAST Isotope I autosampler revealed a potential source of bias for Li isotopic measurement. In the conventional SSB sequence (Blank<sub>1</sub>–LSVEC<sub>1</sub>–Blank<sub>2</sub>–Sample<sub>1</sub>–Blank<sub>3</sub>–LSVEC<sub>2</sub>–Blank<sub>4</sub>–Sample<sub>2</sub>, etc.), the blanks are consistently analyzed in the same loop (configuration 1), while both standards and samples are injected through the other loop. This asymmetric use of the loops may introduce small but systematic bias in measured  $\delta^7\text{Li}$  values, ultimately affecting reproducibility (see Figure 2 main text), likely due to different rinsing (washing) times.

To overcome this limitation, we implemented a modified SSB sequence (Blank<sub>1</sub>–Blank<sub>2</sub>–LSVEC<sub>1</sub>–Blank<sub>3</sub>–Blank<sub>4</sub>–Sample<sub>1</sub>–Blank<sub>5</sub>–Blank<sub>6</sub>–LSVEC<sub>2</sub>, etc.), incorporating two blanks before each standard or sample analysis. This approach alternates the injection of standards and samples between loops A

and B, ensuring balanced use of both loops for all solution types. As shown in Figure 2 (main text), this configuration proved more suitable for low-level lithium analyses ( $\leq 3$  ppb) and improved the reproducibility of lithium isotope measurements. (See Figure 2 main text).

#### *Configuration 1: Conventional SSB sequence*

Blank → Loop A

Standard (LSVEC) → Loop B

Blank → Loop A

Sample → Loop B

(Repeat for all n samples)

#### *Configuration 2 Modified (alternating-loop) SSB sequence*

Blank 1 → Loop A

Blank 2 → Loop B

Standard (LSVEC) → Loop A

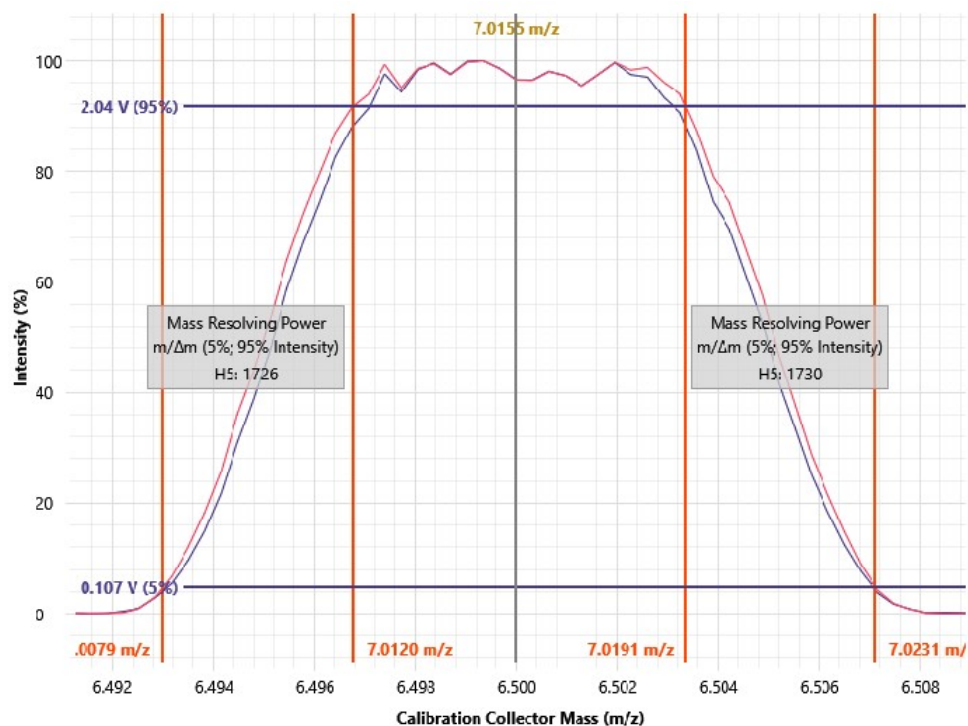
Blank 3 → Loop B

Blank 4 → Loop A

Sample 1 → Loop B

(Repeat alternation for subsequent standards and samples)

#### II. Peak Shape of $^7\text{Li}$ (in red) and of $^6\text{Li}$ (in blue), both normalized to 100% for comparison.



III. Table S1: Compilation of recent seawater values reported in the literature and measured by MC-ICP-MS, excluding Neoma\* data (over the last 10 years)

Area/Name	$\delta^7\text{Li}$ (‰) value	2SD**	N	Li (ppb) MC-ICP-MS	References
NASS-5	30.91	0.26	7	N.R.	(1)
Atlantic Ocean	30.97	0.31	7	50	(2)
NASS-6	30.87	0.15	15	112	(3)
N.R.***	31.2	0.4	19	0.5	(4)
Atlantic Ocean	31.1	0.7	14	20	(5)
Atlantic Ocean	31.1	0.3	6	4	(6)
N.R.	31.27	0.4	30	0.2-0.4	(7)
South China Sea	31.4	0.7	18	80	(8)
AEL, EDM-1-G	31.32	0.83	4	4	(9)
Atlantic Ocean	31.2	0.4	3	20	(10)
Atlantic Ocean	30.88	0.76	4	20	(11)
NASS-6	30.97	0.24	5	1	(12)
N.R.	31.13	0.38	29	0.5	(13)
NASS-7	30.93	0.36	1	5-15	(14)
<p style="text-align: center;"><b>Average</b></p> <p style="text-align: center;"><b><math>31.1 \pm 0.09\text{‰}</math> (2SE, N=14)</b></p> <p style="text-align: center;"><b>2SD = 0.4‰</b></p>					

\*Neoma seawater data published previously are deliberately not included in this table; they are presented in the main text for direct comparison with the Neoma data generated in this study (see Section 6 and Figure 9 main text)

\*\*External reproducibility

\*\*\* Not reported

## References

1. Dellinger M, Gaillardet J, Bouchez J, Calmels D, Louvat P, Dosseto A, et al. Riverine Li isotope fractionation in the Amazon River basin controlled by the weathering regimes. *Geochim Cosmochim Acta*. sept 2015;164:71-93.
2. Toki T, Heshiki S. Improved Method for Seawater Lithium Isotopic Ratio Determination Using. 2015;
3. Lin J, Liu Y, Hu Z, Yang L, Chen K, Chen H, et al. Accurate determination of lithium isotope ratios by MC-ICP-MS without strict matrix-matching by using a novel washing method. *J Anal At Spectrom*. 2016;31(2):390-7.
4. Pogge Von Strandmann PAE, Jones MT, West AJ, Murphy MJ, Stokke EW, Tarbuck G, et al. Lithium isotope evidence for enhanced weathering and erosion during the Paleocene-Eocene Thermal Maximum. *Sci Adv*. 15 oct 2021;7(42):eabh4224.
5. Weynell M, Wiechert U, Schuessler JA. Lithium isotopes and implications on chemical weathering in the catchment of Lake Donggi Cona, northeastern Tibetan Plateau. *Geochim Cosmochim Acta*. sept 2017;213:155-77.
6. Bastian L, Vigier N, Reynaud S, Kerros M, Revel M, Bayon G. Lithium Isotope Composition of Marine Biogenic Carbonates and Related Reference Materials. *Geostand Geoanalytical Res*. sept 2018;42(3):403-15.
7. Bohlin MS, Misra S, Lloyd N, Elderfield H, Bickle MJ. High-precision determination of lithium and magnesium isotopes utilising single column separation and multi-collector inductively coupled plasma mass spectrometry. *Rapid Commun Mass Spectrom*. 30 janv 2018;32(2):93-104.
8. Zhang JW, Meng JL, Zhao ZQ, Liu CQ. Accurate Determination of Lithium Isotopic Compositions in Geological Samples by Multi-collector Inductively Coupled Plasma-Mass Spectrometry. *Chin J Anal Chem*. mars 2019;47(3):415-22.
9. Thibon F, Weppe L, Montanes M, Telouk P, Vigier N. Lithium isotopic composition of reference materials of biological origin TORT-2, DORM-2, TORT-3, DORM-4, SRM-1400 and ERM-CE278k. *J Anal At Spectrom*. 2021;36(7):1381-8.
10. Li X, Han G, Zhang Q, Qu R, Miao Z. Accurate lithium isotopic analysis of twenty geological reference materials by multi-collector inductively coupled plasma mass spectrometry. *Spectrochim Acta Part B At Spectrosc*. févr 2022;188:106348.
11. Golla JK, Bouchez J, Kuessner ML, Rempe DM, Druhan JL. Subsurface weathering signatures in stream chemistry during an intense storm. *Earth Planet Sci Lett*. oct 2022;595:117773.
12. He MY, Deng L, Liu J, Jin ZD, Ren T. High precision measurements of lithium isotopic composition at sub-nanogram by MC-ICP-MS with membrane desolvation. *RSC Adv*. 2023;13(46):32104-9.
13. Krause AJ, Sluijs A, Van Der Ploeg R, Lenton TM, Pogge Von Strandmann PAE. Enhanced clay formation key in sustaining the Middle Eocene Climatic Optimum. *Nat Geosci*. août 2023;16(8):730-8.

14. Cao C, Li T, Chen T, Li G, Li W, Chen J. An efficient Li dual-column system and high-precision Li isotope measurement of high matrix and low-Li samples by MC-ICP-MS. *J Anal At Spectrom.* 2023;38(8):1602-10.